Isolation of a leading order depth imaging series and analysis of its convergence properties

Simon A. Shaw*†, Arthur B. Weglein†, Douglas J. Foster§, Kenneth H. Matson* and Robert G. Keys‡
*BP, †University of Houston, §ConocoPhillips, ‡ExxonMobil

Abstract

The objective of seismic depth imaging is to produce a spatially accurate map of the reflectivity below the Earth's surface. Current methods for depth imaging require an accurate velocity model in order to place reflectors at their correct locations. Existing techniques to derive the velocity model can fail to provide this information with the necessary degree of accuracy, especially in areas that are geologically complex.

Recently, Weglein et al. (2000) have proposed using the inverse scattering series, a direct non-linear inverse procedure, to perform the task of imaging reflectors at depth without needing to specify the exact velocity. The primary objective of the research described here is to derive and develop a practical inverse series algorithm to perform the task of imaging without accurate velocity information. The strategy employed is to isolate a subseries of the inverse series with the purpose of imaging reflectors in space (Weglein et al., 2002).

In this paper, a leading order imaging subseries is isolated and its convergence properties are analyzed. It is shown analytically that this imaging subseries converges for any finite contrast between the actual and reference medium, and for band-limited data with a finite maximum frequency. The rate of convergence is greater for small contrasts and smaller maximum frequencies.

1 Introduction

At its core, seismic data processing is an inverse method; the data are inverted for the Earth's subsurface properties. These properties include the spatial location of reflectors and the contrasts in density and elastic properties at these reflectors. In practice, the processing of seismic data is carried out in a sequence of steps, e.g., random noise attenuation, source wavelet deconvolution, removal of free surface multiples, removal of internal multiples, imaging (also called migration), and inversion for changes in Earth properties. The order in which these steps are carried out can be important because most algorithms assume that the data have been preconditioned by the preceding processes. The research described here concerns the single step of imaging primaries. Primaries are events in the measured wavefield that have experienced a single upward reflection in the subsurface and are distinguished from multiples which have experienced more than one upward reflection. Imaging may be thought of as a process that transforms the recorded primary seismic wavefield into a spatially accurate picture of the Earth's subsurface reflectivity.

The research described here represents progress in a long-term project to develop multi-dimensional algorithms that have a greater ability to achieve the goals of seismic processing while lowering the demands on (often inaccessible) a-priori information about the subsurface. As with earlier analysis of algorithms for multiple attenuation, the evaluation of new concepts and theory progresses from simple, analytic examples to complex, numerical models and ultimately to field data. To avoid numerical, stability or discreteness issues, testing is first conducted with analytic data for one-dimensional examples. This ensures that the results are attributed to the inverse procedure only.

The following section explains the motivation for addressing the problem of imaging when the exact velocity model is unknown. Then, in the next section, the inverse scattering series is derived and the strategy for isolating subseries of the inverse series that perform seismic processing tasks is described. In the remaining sections, a leading order imaging subseries is derived and its convergence properties are studied analytically and numerically.

2 Motivation for an accurate imaging algorithm when the velocity is unknown

Reflectors exist where there are sharp contrasts in Earth material properties that are usually attributed to boundaries between different types of rocks and fluids. Oil and gas are often trapped below the surface by impermeable rocks. Seismic imaging produces a map of subsurface reflectors. The accuracy of this reflector map has a direct impact on our ability to predict the location, volume and even type of hydrocarbons trapped below the surface. Hence seismic imaging plays a key role in exploration and production of natural resources.

Current methods for imaging can be derived using Green's Theorem and the wave equation to predict the wavefield inside the Earth from measurements on its surface (e.g., Schneider 1978; Stolt 1978; Berkhout and Palthe 1981; Wapenaar et al. 1989). For example, for a constant density acoustic medium, if P is the wavefield due to the seismic source, and G is

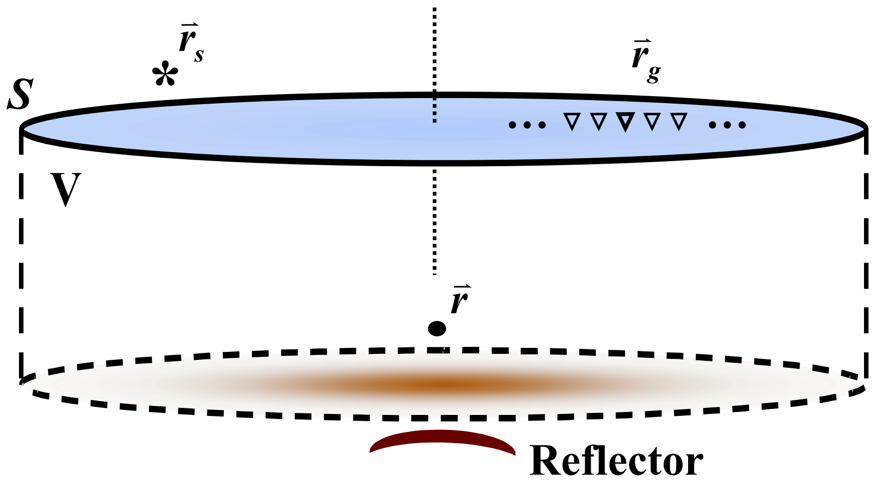

Figure 1: Current imaging algorithms may be derived using Green's Theorem and the wave equation to predict the wavefield in the Earth from measurements on its surface. Knowledge of the Earth's properties inside the volume V is required.

the Green's function that satisfies

$$\left(\nabla^2 + \frac{\omega^2}{c^2(\vec{r})}\right) G(\vec{r}|\vec{r}\,';\omega) = \delta(\vec{r} - \vec{r}\,'), \tag{1}$$

where c is the velocity inside the volume V defined in Figure 1, then the wavefield prediction formula can be shown to be

$$P(\vec{r}|\vec{r}_s;\omega) = \oint_{\vec{r}\,' \in S} \left(P(\vec{r}\,'|\vec{r}_s;\omega)\nabla G(\vec{r}|\vec{r}\,';\omega) - G(\vec{r}|\vec{r}\,';\omega)\nabla P(\vec{r}\,'|\vec{r}_s;\omega)\right) \cdot \hat{n} dS \tag{2}$$

where $\vec{r}$ is the location at which the wavefield is predicted and $\vec{r}_s$ is the source location. The need for the measurement of ∇P is avoided by making G satisfy Dirichlet boundary conditions on the measurement surface. The requirement of current imaging algorithms for the velocity comes from the need to compute the Green's function G inside the volume V.

The wavefield predicted in the Earth is transformed into a map of reflectivity using an imaging condition. Usually, the imaging condition asks for the seismic amplitude recorded in the limit of a small recording time for a hypothetical experiment where a source and receiver are coincident in the Earth (e.g., Claerbout 1971). If a reflector exists immediately below the source and receiver in the Earth, then the imaging condition will output a measure of the reflector's strength.

As mentioned, traditional methods for imaging require the precise velocity model in order to compute the Green's function that back-propagates the measured wavefield into the Earth.

Without the true propagation velocity, the wavefield in the Earth will not be correctly predicted, and the imaging condition will fail to locate the reflectors. It is for this reason that the quality of the results from current methods for depth imaging are critically dependent on the accuracy of the velocity model.

Velocity information itself can be derived from seismic reflection data by picking reflection travel times (Taner and Koehler, 1969) or using reflection tomography (e.g., Stork and Clayton 1991). In practice, the seismic interval velocities can be in error by 5-10% (Gray et al., 2001) depending on data quality, geologic complexity, and the sophistication and robustness of the algorithm being used to derive them.

The failure of current methods to produce accurate depth images below complex overburdens, such as below salt, basalt, and karsted or gas-saturated sediments, is the motivation for the research proposed here. Under these geologic conditions, current velocity estimation procedures fail to yield the velocity model with the necessary degree of accuracy to place reflectors at their correct locations. The objective of this research is to develop a new method to accurately image seismic data that is less dependent on our ability to describe the precise velocity model.

3 Scattering theory and seismic data processing

The research described here applies inverse scattering theory to the seismic inverse problem. In scattering theory, the difference in the behavior of an incident wave in two media (referred to as the *reference* medium and the *actual* medium) is described in terms of the difference between the physical properties of these two media.

The wave equations for the actual and reference wavefields are expressed by

$$L\psi = A(\omega)\delta(\vec{r}_g - \vec{r}_s) \tag{3}$$

$$L_0\psi_0 = A(\omega)\delta(\vec{r}_g - \vec{r}_s) \tag{4}$$

where L and L_0 are the differential operators that describe wave propagation in the actual and reference media, respectively, and $A(\omega)$ is the source wavelet. The variables $\vec{r}_g$ and $\vec{r}_s$ are the receiver and source position vectors, respectively. The Green's functions for the actual medium, G, and the reference medium, G_0, satisfy

$$LG = \delta(\vec{r}_g - \vec{r}_s) \tag{5}$$

$$L_0G_0 = \delta(\vec{r}_g - \vec{r}_s) \tag{6}$$

and so $\psi = A(\omega)G$ and $\psi_0 = A(\omega)G_0$. The scattering potential and the scattered wavefield are defined by

$$V \equiv L_0 - L \tag{7}$$

$$\psi_s \equiv \psi - \psi_0, \tag{8}$$

respectively. The equation that relates the actual and reference wavefields to the scattering potential is the Lippmann-Schwinger equation

$$\psi(\vec{r}_g|\vec{r}_s;\omega) = \psi_0(\vec{r}_g|\vec{r}_s;\omega) + \int_{-\infty}^{\infty} G_0(\vec{r}_g|\vec{r}\,';\omega)V(\vec{r}\,';\omega)\psi(\vec{r}\,'|\vec{r}_s;\omega)d\vec{r}\,'. \tag{9}$$

This equation can be successively iterated for ψ on the right-hand side resulting in the forward, or Born, series for the actual wavefield ψ

$$\psi = \psi_0 + \psi_1 + \psi_2 + \dots \tag{10}$$

where

$$\psi_1(\vec{r}_g|\vec{r}_s;\omega) = \int_{-\infty}^{\infty} G_0(\vec{r}_g|\vec{r}\,';\omega)V(\vec{r}\,';\omega)\psi_0(\vec{r}\,'|\vec{r}_s;\omega)d\vec{r}\,' \tag{10a}$$

$$\psi_2(\vec{r}_g|\vec{r}_s;\omega) = \int_{-\infty}^{\infty} G_0(\vec{r}_g|\vec{r}\,';\omega)V(\vec{r}\,';\omega) \times \int_{-\infty}^{\infty} G_0(\vec{r}\,'|\vec{r}\,'';\omega)V(\vec{r}\,'';\omega)\psi_0(\vec{r}\,''|\vec{r}_s;\omega)d\vec{r}\,'\,d\vec{r}\,'' \tag{10b}$$

$$\vdots$$

The forward series is a solution for ψ in terms of G_0, ψ_0 and V. The wavefield that propagates in the *actual* medium is described in terms of an infinite series of propagations in a chosen *reference* medium and interactions with the potential V. Conversely, the inverse series is a solution for V in terms of the scattered field on the measurement surface $(\psi - \psi_0)_m = (\psi_s)_m$ and G_0. The inverse series can be derived by first writing V as the sum of constituent components (Moses, 1956)

$$V = V_1 + V_2 + V_3 + \dots = \sum_{n=1}^{\infty} V_n \tag{11}$$

where V_n is the portion of V that is n^{th} order in the measured values of the scattered field, $(\psi_s)_m$. Substitution of equation (11) into the forward series (equation 10) and matching terms that are equal order in $(\psi_s)_m$ yields the inverse series:

$$(G_0V_1\psi_0)_m = (\psi_s)_m \tag{11a}$$

$$(G_0V_2\psi_0)_m = -(G_0V_1G_0V_1\psi_0)_m \tag{11b}$$

$$(G_0V_3\psi_0)_m = -(G_0V_1G_0V_1G_0V_1\psi_0)_m - (G_0V_2G_0V_1\psi_0)_m - (G_0V_1G_0V_2\psi_0)_m \tag{11c}$$

$$\vdots$$

See, for example, Weglein et al. (1981) for references to the development of the inverse series. To calculate only the first term in the inverse series (i.e., solving equation 11a) and to treat $V_1 \approx V$ is to make the inverse Born approximation. However, the inverse series does not make that assumption. V_1 is assumed to be the first order approximation to V and equation (11a) is the exact equation for that quantity. The inverse Born approximation forms the basis of all current techniques employed to perform seismic inversion (Clayton and Stolt, 1981), i.e., normal moveout (NMO) stack, amplitude variation with offset (AVO) analysis, migration (imaging) and migration-inversion (Stolt and Weglein, 1985). Linear approximate inverse methods are also the basis of medical imaging and other non-destructive evaluation methods. For the seismic problem, the inverse Born is a reasonable approximation for precritical primary reflections, for small contrasts in material properties, and for a reference medium that is close to the actual medium. Second and higher terms in the inverse series can be viewed as correcting V_1 towards V when the series convergences. The tasks of removing multiples, imaging primaries at their correct depth, and inverting for large changes in Earth properties reside in the second and higher order terms in the inverse series.

The inverse scattering series (equation 11) is a multi-dimensional direct inversion procedure. The scattering medium's properties are directly determined from the recorded data without iterative updating of the reference medium towards the actual medium. Alternative approaches, e.g., iterative linear inversion, involve updating the reference model so that the reference wavefield, in some sense, fits the observed data (Tarantola, 1987). The inverse series is a distinct and separate method from iterative linear inversion. Equation (11) solves for $V_1, V_2 \ldots$ and hence for $V = V_1 + V_2 + \ldots$ directly in terms of $(\psi_s)_m$ and G_0.

Empirical tests of the *entire* inverse series for a simple acoustic model suggested that it does not converge for contrasts between actual and reference medium properties greater than about 11 % (Carvalho, 1992). Based on these tests, it was believed that the radius of convergence is too small to be of direct practical use when no a-priori information is supplied. Rather than abandon the inverse series, research has been undertaken to isolate convergent subseries that perform individual tasks associated with inversion. Inversion of seismic data can be viewed as performing a sequence of four tasks:

1. Removal of free-surface multiples;
2. Removal of internal multiples;
3. Positioning reflectors at their correct spacial locations (imaging); and
4. Inverting reflectivity for changes in Earth parameters (target identification).

The inverse series accomplishes these tasks using only measured data and reference medium properties. Isolating specific subseries that perform these tasks is less ambitious than directly inverting for Earth properties in one step and so convergence properties may be more favorable. Also, by carrying out these tasks in sequence, tasks 2–4 benefit from the fact that previous tasks have already been performed which constitutes valuable *a priori* information. At each step, the simplest possible reference medium is chosen that allows rapid convergence of the specific subseries.

This strategy of task separation first produced a multi-dimensional free surface multiple removal algorithm. Free surface multiples are events that have reflected in the subsurface, traveled back up, hit the free surface at least once, and traveled back into the Earth. These events usually have large amplitudes and can obscure reflection events that have traveled further into the Earth but arrive at the same time as the multiples. The presence of multiples often precludes accurate estimation of reference medium properties. The second task-specific subseries to be isolated was the one that predicts and attenuates internal multiple reflections. Internal multiples are events that have all their downgoing reflections below the free surface.

The multiple removal algorithms derived using the inverse series (Weglein et al., 1997) have the unique property that they expect the recorded seismic data and the source wavelet as input, but do not require the propagation velocity or any other subsurface information. For marine seismic data, both the free surface and internal multiple subseries converge for a homogeneous acoustic reference medium – water – which makes the algorithms computationally efficient. More importantly, they predict and attenuate multiples generated by actual Earth model types that are much more complicated than the homogeneous acoustic reference medium and include elastic, heterogeneous, anisotropic and certain forms of anelastic media.

An important prerequisite of these inverse scattering algorithms is knowledge of the source wavelet. Methods for estimating the wavelet include direct near-field measurements (Ziolkowski, 1991) or an estimation from the recorded data (Weglein and Secrest, 1990; Osen et al., 1998; Tan, 1999).

The strategy employed in this research is to first remove the multiples with their task-specific subseries, and then to use the demultipled data with its source wavelet deconvolved, as input to the subseries that act on primaries. This represents a staged approach where tasks are carried out in an order that progresses from relatively easy to more challenging and that uses the successful completion of earlier tasks to improve the chances of subsequent tasks being successful.

Recently, Weglein et al. (2000) have proposed using the inverse scattering series to perform the third and fourth tasks of imaging reflectors in depth and inverting for Earth parameters, both in terms of reference medium information. The concepts surrounding the task of imaging using the inverse series have been set out by Weglein et al. (2002). The next section summarizes how the inverse series performs imaging illustrated using 1-D analytic and numerical examples.

4 Imaging using the inverse series

4.1 1-D inverse series and task separation

Wave propagation in a 1-D constant density variable velocity acoustic medium is described by the equation

$$\left(\frac{d^2}{dz^2} + k^2(z)\right)\psi(z;\omega) = 0 \tag{12}$$

where $k(z) = \omega/c(z)$, ω is the angular frequency, $c(z)$ is the velocity, and z is the field point of the wavefield. Assume that the region that equation (12) describes does not contain the source. If the reference medium is chosen to be an acoustic wholespace with velocity c_0, then the perturbation has the form

$$\begin{aligned} V &= L_0 - L \\ &= k_0^2 - k^2 \\ &= k_0^2\alpha \end{aligned} \tag{13}$$

where $\alpha(z) = 1 - c_0^2/c^2(z)$ and $k_0 = \omega/c_0$. In this context, the inverse problem is to solve for α where

$$\alpha = \alpha_1 + \alpha_2 + \alpha_3 + \ldots = \sum_{n=1}^{\infty} \alpha_n \tag{14}$$

The first term in the inverse series (equation 11a) is then

$$\psi_s(z_m;\omega) = \int_{-\infty}^{\infty} \frac{e^{ik_0|z_m-z'|}}{2ik_0} k_0^2 \alpha_1(z')\psi_0(z';k_0)dz' \tag{15}$$

where z_m is the measurement depth and the reference wavefield is $\psi_0 = e^{ik_0(z'-z_m)}$. Solving for α_1 (see appendix 6) yields

$$\alpha_1(z) = 4\int_0^z \psi_s(z_m;z')dz' \tag{16a}$$

where $z' = c_0t/2$ and t is the travel time. Time zero ($t = 0$) corresponds to when the downgoing incident wave passes z_m. Equation (16a), which in this 1-D case amounts to trace integration, is a conventional migration-inversion. The second term in the inverse series (Equation 11b) can be broken up in to two terms (see appendix 6):

$$\alpha_2(z) = -\frac{1}{2}\left(\alpha_1^2(z) + \left[\frac{d\alpha_1(z)}{dz}\right]\int_0^z \alpha_1(z')dz'\right). \tag{16b}$$

These two terms in α_2 correspond to "self-interaction" (α_1^2) and "separated" ($\alpha_1' \int \alpha_1$) scattering diagrams represented in Fig. 2. All higher order inverse series terms can be broken up in a similar manner. As has been reported by Weglein et al. (2002), separated diagram terms with a single upward scattering point contribute to a subseries that images reflectors at their correct spatial location, and self-interaction terms form the subseries that corrects the amplitude of α_1 towards α. The third term in the inverse series (Equation 11c) is broken up as follows (see appendix 6):

$$\begin{aligned}\alpha_3(z) =& \frac{3}{16}\alpha_1^3(z) + \frac{1}{8}\left[\frac{d^2}{dz^2}\alpha_1(z)\right]\left(\int_0^z \alpha_1(z')dz'\right)^2 \\ &- \frac{1}{8}\left[\frac{d}{dz}\alpha_1(z)\right]\int_0^z \alpha_1^2(z')dz' \\ &+ \frac{3}{4}\left[\frac{d}{dz}\alpha_1(z)\right]\alpha_1(z)\int_0^z \alpha_1(z')dz' \\ &- \frac{1}{16}\int_0^z\int_0^z \left[\frac{d}{dz'}\alpha_1(z')\right]\left[\frac{d}{dz''}\alpha_1(z'')\right]\alpha_1(z''+z'-z)dz''dz'\end{aligned} \tag{16c}$$

Consider that the inverse series can be separated into subseries so that

$$\begin{aligned}\alpha &= \alpha_1 + \alpha_2 + \alpha_3 + \ldots \\ &= \alpha_1 + \left(\alpha^{IS} - \alpha_1\right) + \left(\alpha^{AO} - \alpha_1\right) + \left(\alpha^{IM} - \alpha_1\right) + \ldots\end{aligned} \tag{17}$$

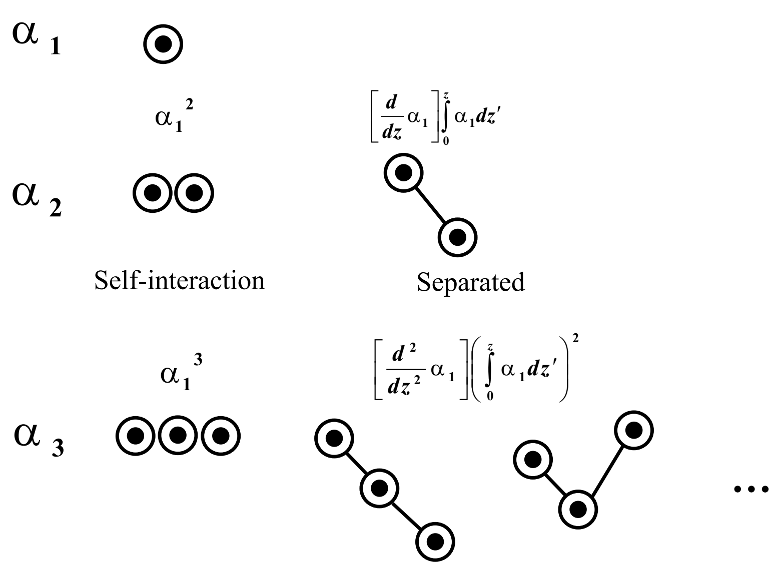

Figure 2: The terms in the inverse series can be interpreted using scattering diagrams. The circles represent α_1 and the line represents a propagation in the reference medium. Self-interaction occurs when two or more scattering points are at the same location. Separated diagrams refer to scattering between points that are at different locations. Diagrams shown here perform inverse tasks on primary events.

where

$$\begin{aligned}\alpha^{IS} &= \text{Imaging subseries}\\ \alpha^{AO} &= \text{Subseries that inverts amplitudes only}\\ \alpha^{IM} &= \text{Subseries that removes internal multiples}\end{aligned}$$

(Note that each of the subseries in equation (17) have been written to include α_1.)

The residual "$+\ldots$" in equation (17) includes terms that correct the amplitude between where α_1 places reflectors, and where α^{IS} locates them. Coupled tasks such as these will be the subject of future reports.

The removal of internal multiples begins in the third term in the inverse series (Weglein et al., 1997) and, in this context, is written

$$\alpha^{IM}(z) = \alpha_1(z) - \frac{1}{16}\int_0^z \int_0^z \left[\frac{d}{dz'}\alpha_1(z')\right]\left[\frac{d}{dz''}\alpha_1(z'')\right]\alpha_1(z''+z'-z)dz''dz' + \ldots \tag{18}$$

The self-interaction terms that correct amplitude only, and not location, can be grouped and written

$$\alpha^{AO}(z) = \alpha_1(z) - \frac{1}{2}\alpha_1^2(z) + \frac{3}{16}\alpha_1^3(z) - \ldots \tag{19}$$

The imaging subseries terms do not alter the amplitude of α_1 but act to correctly locate the interfaces that are mislocated in α_1. The imaging subseries can be considered in two parts: leading order (LO) and higher order (HO) contributions. Leading order terms are those that correspond to purely separated scattering diagrams with a single upward scattering point, whereas the higher order imaging terms consist of separated diagrams that also have self-interaction components (see Fig. 3) above the deepest scattering point.

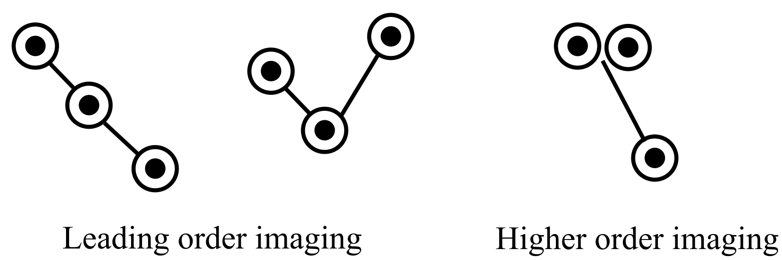

Figure 3: Examples of leading order and higher order imaging terms from the third term in the inverse series.

$$\alpha^{IS}(z) = \alpha^{IS_{LO}}(z) + \alpha^{IS_{HO}}(z) \tag{20}$$

More will be said about the leading and higher order contributions in the next section with an analytic example. The leading order contributions to the imaging subseries are

$$\begin{aligned}\alpha^{IS_{LO}}(z) =& \alpha_1(z) - \frac{1}{2}\left[\frac{d\alpha_1(z)}{dz}\right]\left(\int_0^z \alpha_1(z')dz'\right) \\ &+ \frac{1}{8}\left[\frac{d^2\alpha_1(z)}{dz^2}\right]\left(\int_0^z \alpha_1(z')dz'\right)^2 + \ldots \\ =& \sum_{n=0}^{\infty}\left(\frac{(-1/2)^n}{n!}\right)\left[\frac{d^n\alpha_1(z)}{dz^n}\right]\left(\int_0^z \alpha_1(z')dz'\right)^n\end{aligned} \tag{21}$$

Equation (21) is the leading order imaging subseries and was originally derived through an analysis of the first three terms in the inverse series, and the recognition of a general form that predicts the expected fourth and higher order series coefficients in the case of a simple analytic example (given in the next section). This analysis is typical of the kind used to derive inverse series algorithms in the past. The forward series gives us clues as to which terms in the inverse series perform a particular task. Then we isolate those terms of the inverse series and study their behavior for simple analytic examples deliberately chosen so that the inverse task is clear. For the task of imaging, a logical example to study a two-interface model where we only know the velocity to the first interface. The first term in the inverse series will properly locate the shallower interface and mislocate the deeper one. If the series converges, then the higher order terms will neccesarily act to correct the depth of the deeper interface. It was this type of analysis that yielded the leading order imaging algorithm, which was subsequently tested on more complicated analytic and numerical examples with good results.

In the next two sections, analytic and numerical examples are used to illustrate how this algorithm works. Notice that equation (21) can be simplified as follows

$$\alpha^{IS_{LO}}(z) = \sum_{n=0}^{\infty}\left(\frac{(-1/2)^n}{n!}\right)\left[\frac{1}{2\pi}\int_{-\infty}^{\infty}(ik_0)^n\tilde{\alpha}_1(k_0)e^{ik_0z}dk_0\right]\left(\int_0^z \alpha_1(z')dz'\right)^n$$
$$=\frac{1}{2\pi}\int_{-\infty}^{\infty}\sum_{n=0}^{\infty}\frac{1}{n!}\left(-ik_0\frac{1}{2}\int_0^z \alpha_1(z')dz'\right)^n \tilde{\alpha}_1(k_0)e^{ik_0z}dk_0.$$

Recognizing that

$$\sum_{n=0}^{\infty}\frac{1}{n!}\left(-ik_0\frac{1}{2}\int_0^z \alpha_1(z')dz'\right)^n = \exp\left(-ik_0\frac{1}{2}\int_0^z \alpha_1(z')dz'\right) \tag{22}$$

for any finite k_0 and $\int_0^z \alpha_1 dz'$, then we can write a closed form of the leading order imaging subseries

$$\alpha^{IS_{LO}}(z) =\frac{1}{2\pi}\int_{-\infty}^{\infty}\tilde{\alpha}_1(k_0)e^{ik_0\left(z-\frac{1}{2}\int_0^z \alpha_1(z')dz'\right)}dk_0 \tag{23}$$

$$=\alpha_1\left(z-\frac{1}{2}\int_0^z \alpha_1(z')dz'\right) \tag{24}$$

Equation (23) has the form of a phase-shift migration, where the shift is equal to $\frac{1}{2}\int_0^z \alpha_1(z')dz'$. In the absence of the actual velocity function, this algorithm extracts the neccesary information from the amplitudes and depth information in α_1 through an integral. The closed form expression will be used to discuss the convergence properties after the analytic and numerical examples.

4.2 Analytic example

In this section, the ability of the inverse series to perform the task of imaging without needing to specify the velocity is illustrated using a simple 1-D acoustic example. Consider the experiment illustrated in Figure 4 with a source and receiver at the surface $z_m = 0$. The reference velocity is chosen to be constant c_0, whereas the actual Earth velocity is an unknown function $c(z)$.

Figure 4: A single layer with velocity c_1 between two homogeneous half-spaces with velocity c_0 and c_2. The depth of the first interface is z_a and the depth of the second interface is z_b.

In accordance with the strategy, all multiples (i.e., free-surface and internal multiples) have been removed from the input data. Hence, for this example, the data consist of two primary reflections that arrive at times t_1 and t_2

$$D(t) = R_1\delta(t - t_1) + \hat{R}_2\delta(t - t_2). \tag{25}$$

R_1 is the reflection coefficient for a downgoing wave at the first interface and $\hat{R}_2 = T_{01}R_2T_{10}$ where R_2 is the downgoing reflection coefficient at the second interface and T_{01} and T_{10} are the transmission coefficients for a wave propagating down and up, respectively through the first interface. The equations for the reflection and transmission coefficients are

$$R_1 = \frac{c_1 - c_0}{c_1 + c_0} \tag{26}$$

$$T_{01} = 1 - R_1 \tag{27}$$

$$T_{10} = 1 + R_1 \tag{28}$$

$$\text{and } R_2 = \frac{c_2 - c_1}{c_2 + c_1}. \tag{29}$$

The data D differ from the scattered field ψ_s in equation (16a) in that multiples having been removed from D. Substitution of equation (25) into equation (16a) yields a primaries-only α_1:

$$\alpha_{1_p}(z) = 4R_1H(z - z_a) + 4\hat{R}_2H(z - z_{b'}) \tag{30}$$

where $z_{b'}$ is the pseudo depth at which the event with travel time t_2 images with velocity c_0. This pseudo depth can be written

$$z_{b'} = z_a + \gamma(z_b - z_a) \tag{31}$$

where $\gamma = c_0/c_1$. Figure 5 illustrates α_1 for the case where $c_0 < c_1$. The second reflector is imaged at a depth that is too shallow because the reference velocity is less than the actual velocity in the layer. Furthermore, the amplitude of α_1 is different from that of α. These differences between α_1 and α are corrected by the higher order terms in the inverse series.

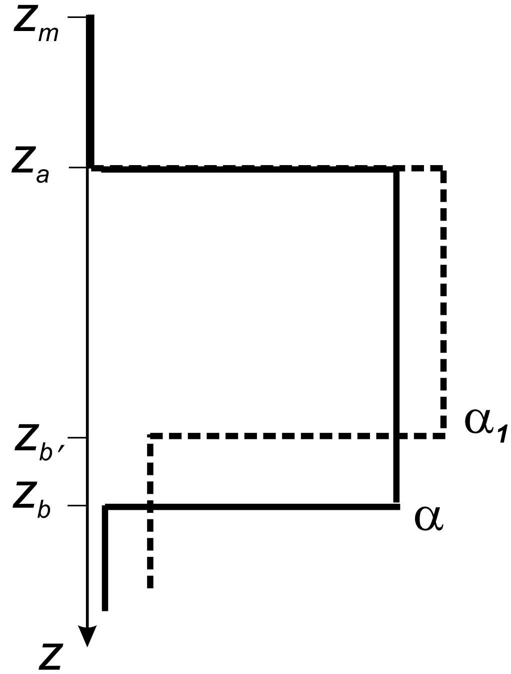

Figure 5: Given the reference velocity c_0, the first term in the inverse series, α_1, places the second interface at the incorrect depth $z_{b'}$ rather than the actual depth z_b. For the case where $c_0 < c_1$, $z_{b'}$ will be shallower than z_b. The task of imaging is the process of moving the interface from $z_{b'}$ to z_b whereas the last remaining task in the inversion for α must correct the amplitude of α_1. Both of these tasks reside in the higher order terms of the inverse series.

Evaluating the second and higher order terms in the leading order imaging subseries (equation 21) leads to

$$\alpha_{2_p}^{IS_{LO}}(z) = -\,2R_1(z-z_a)4\hat{R}_2\delta(z-z_{b'}) \tag{32}$$
$$\alpha_{3_p}^{IS_{LO}}(z) = 2R_1^2(z-z_a)^2 4\hat{R}_2\delta'(z-z_{b'}) \tag{33}$$
$$\alpha_{4_p}^{IS_{LO}}(z) = -\,\frac{4}{3}R_1^3(z-z_a)^3 4\hat{R}_2\delta''(z-z_{b'}) \tag{34}$$
$$\vdots$$

In this example, the task of imaging is to shift the deeper interface from $z_{b'}$ to z_b. The imaging subseries accomplishes this shift through a Taylor series for the difference of two Heaviside functions expanded about the mislocated interface. This shift is a scaled box $B(z)$ where

$$\begin{aligned} B(z) =& H(z-z_{b'}) - H(z-z_b) \\ =& (z_b-z_{b'})\delta(z-z_{b'}) - \frac{(z_b-z_{b'})^2}{2!}\delta'(z-z_{b'}) + \frac{(z_b-z_{b'})^3}{3!}\delta''(z-z_{b'}) - \dots \end{aligned} \tag{35}$$

The δ functions and their derivatives relate to those in equations (32)–(34). The coefficients of the Taylor series contain the correct depth to the interface, z_b. In the inverse series, these coefficients are constructed order by order in the data D, and are a function of the amplitudes and travel times (or pseudo depths) down to the reflector being imaged. Combining equations (26) and (31) provides the coefficients

$$(z_b-z_{b'}) = -\,2\,(z_{b'}-z_a)\left(R_1+R_1^2+R_1^3+\dots\right) \tag{36}$$
$$\frac{(z_b-z_{b'})^2}{2!} = 2\,(z_{b'}-z_a)^2\left(R_1^2+2R_1^3+3R_1^3+\dots\right) \tag{37}$$
$$\frac{(z_b-z_{b'})^3}{3!} = -\,\frac{4}{3}\,(z_{b'}-z_a)^3\left(R_1^3+3R_1^4+6R_1^5+\dots\right) \tag{38}$$
$$\vdots$$

The contributions to these coefficients that are *leading order* in the data are

$$(z_b-z_{b'})^{LO} = -\,2\,(z_{b'}-z_a)\,R_1 \tag{39}$$
$$\left(\frac{(z_b-z_{b'})^2}{2!}\right)^{LO} = 2\,(z_{b'}-z_a)^2\,R_1^2 \tag{40}$$
$$\left(\frac{(z_b-z_{b'})^3}{3!}\right)^{LO} = -\,\frac{4}{3}\,(z_{b'}-z_a)^3\,R_1^3 \tag{41}$$
$$\vdots$$

These coefficients correspond to those predicted by the leading order imaging subseries terms in equations (32)–(34). The higher order imaging subseries terms predict the remaining coefficients in equations (36)–(38). For $|R_1| << 1$ the leading order contributions will be more significant than the higher order ones. Careful analysis of the relative significance of these terms will be the subject of future work.

In the next subsection, numerical examples illustrate how the imaging subseries terms act to shift the reflectors towards the correct depth for band-limited synthetic input data.

4.3 Numerical Examples

Consider the 1-D model depicted in Fig. 4 with the following parameters: c_0 =2000 m/s, c_1 =2200 m/s, c_2 =2020 m/s, z_a =100 m and z_b=140m. Choosing a reference velocity c_0 =2000 m/s, and simulating data for a $0-125$ Hz band-limited source, then the computed α_1 is shown as the dashed red line in Fig. 6.

The depth that the reference velocity images the second reflector at is $z_{b'}$=136m. The band-limited singular functions of the imaging subseries act to extend the interface from $z_{b'}$ to z_b. The cumulative sum of these imaging subseries terms is illustrated in Fig. 7. After summing five terms, the imaging subseries has converged and the deeper reflector has moved towards its correct depth z_b.

Figure 8 illustrates the result of the closed form of the leading order imaging subseries for a four-layer example. For this example, the leading order contributions to the imaging series are seen to shift the interfaces (in α_1) most of the distance towards their actual depths.

5 Convergence properties of the leading order imaging subseries

The essence of the leading order imaging series for the 1-D acoustic case has been shown to reduce to the Taylor series for e^x (equation 22), i.e.,

$$e^x = \sum_{n=0}^{\infty} \frac{x^n}{n!} \tag{42}$$

where

$$x = \left(-ik_0 \frac{1}{2} \int_0^z \alpha_1(z')dz'\right). \tag{43}$$

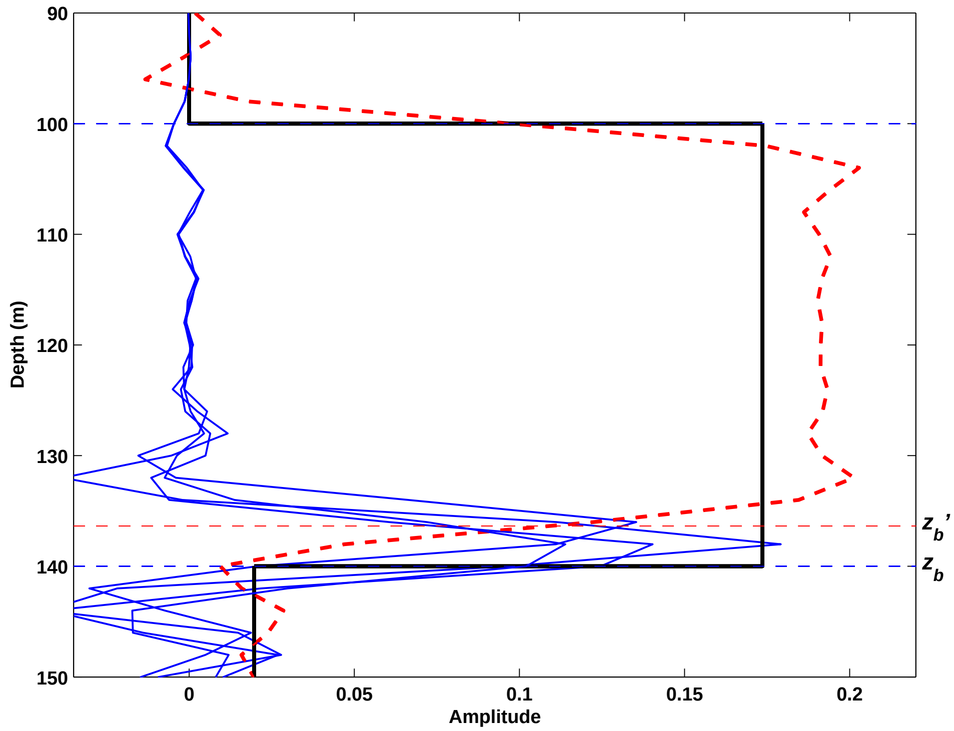

Figure 6: Five terms in the leading order imaging subseries. The solid black line is the actual perturbation α and the dashed red line is α_1, the first approximation to α. The blue lines are the leading order imaging subseries terms. The cumulative sum of these imaging terms is shown in Fig. 7.

k_0 is the reference wavenumber (ω/c_0) and α_1 is a migration-inversion, or linear estimate of α.

This series for e^x is known to converge for any finite x, and hence the leading order imaging subseries will converge as long as both the maximum frequency ω, and the "cumulative" perturbation are both finite. Both of these conditions are realizable in practice.

Concerning the rate of convergence, the series will converge more rapidly for smaller perturbations and for smaller values of ω. Hence, the closer the reference medium velocity is to the actual medium velocity, the faster the series will converge. Since the strategy is to remove multiples before processing primaries, then velocity analysis can be employed to derive a velocity model that is proximate to the actual model, thereby making the contrast between the reference medium and the actual medium as small as possible. Also, lower resolution data (small ω) will image more quickly using this imaging series.

As might be expected, the leading order imaging subseries will not converge to the exact

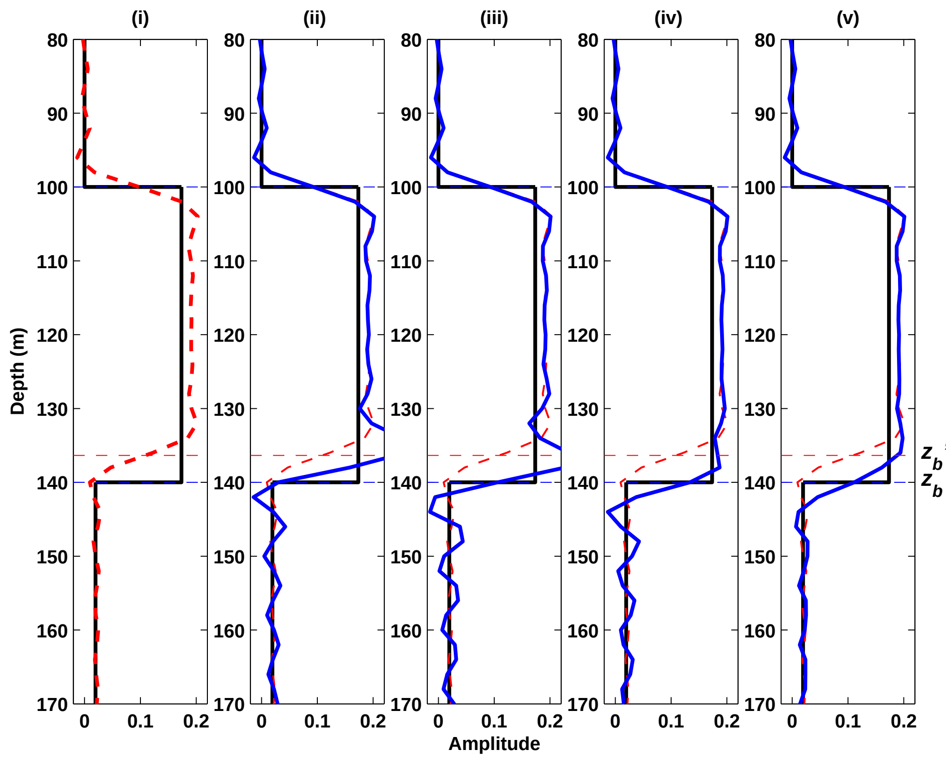

Figure 7: Cumulative sum of five terms in the leading order imaging subseries. The solid black line is the perturbation α and the red line is the first approximation to α or the first term in the inverse series, α_1. The blue line is the cumulative sum of the imaging subseries terms, e.g. in panel (ii) the sum of two terms in the subseries is shown, and in panel (v) the sum of five terms in the subseries is displayed.

depth because the higher order terms are not included in the series. Returning to the simple analytic example in Fig. 4, where the data is expressed by Eq. (25), then Eq. (24) provides for the leading-order imaged data:

$$\begin{aligned}\alpha_p^{IS_{LO}} =& 4R_1 H\left(z - 2R_1(z-a)H(z-a) - a - 2\hat{R}_2(z - z_{b'})H(z - z_{b'})\right)\\ &+ 4\hat{R}_2 H\left(z - 2R_1(z-a)H(z-a) - b' - 2\hat{R}_2(z - z_{b'})H(z - z_{b'})\right) \end{aligned} \tag{44}$$

Studying this expression, we find that for $|R_1| < 1/2$

$$\alpha_p^{IS_{LO}} = 4R_1 H\left(z - a\right) + 4\hat{R}_2 H\left(z - b^{LO}\right) \tag{45}$$

where the second interface has shifted from b' to the leading order approximation to b,

$$b^{LO} = a + \frac{(b' - a)}{(1 - 2R_1)}. \tag{46}$$

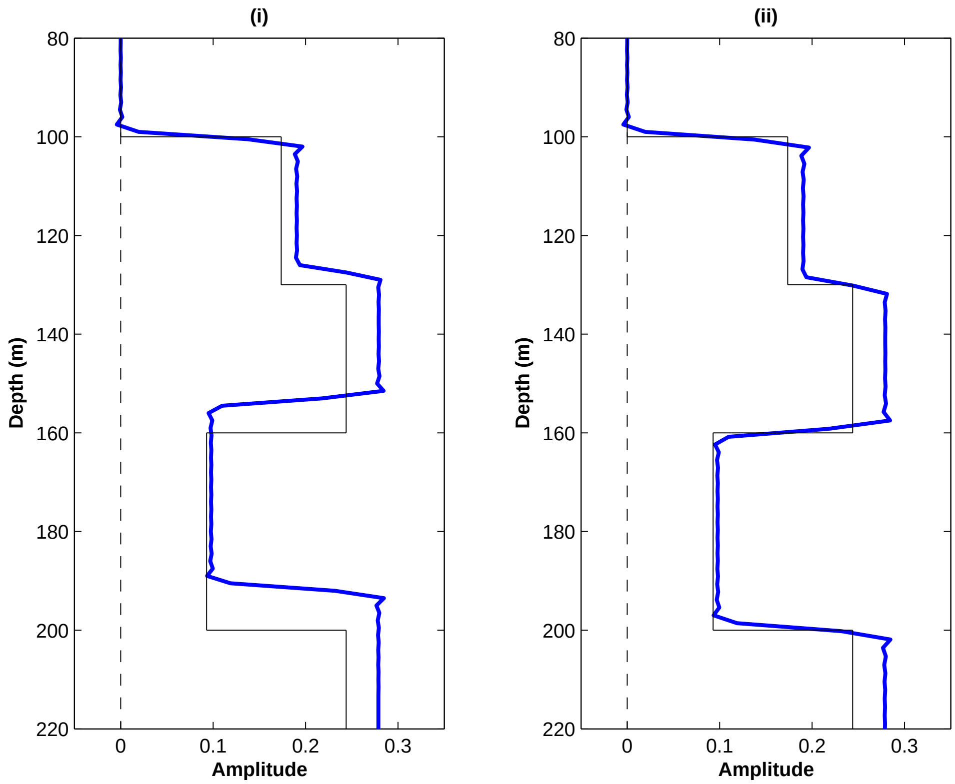

Figure 8: The thin black line shows α for a four layer example where $c_0 = 1500$ m/s, $c_1 = 1650$ m/s, $c_2 = 1725$ m/s, $c_3 = 1575$ m/s and $c_4 = 1725$ m/s. The thick blue line in panel (i) is α_1 generated using the constant velocity $c_0 = 1500$ m/s for 0-125 Hz band-limited synthetic data. The thick blue line in panel (ii) shows the closed form result of the leading order imaging subseries $\alpha_p^{IS_{LO}}$. The interfaces have shifted from the incorrect depths towards their correct ones.

The actual depth b is (from equation 31)

$$b = a + \frac{(1 - R_1)}{(1 + R_1)}(b' - a). \tag{47}$$

For small R_1, b^{LO} is a good approximation to b. Analysis of more complicated analytic examples, including the effects of transmission in the overburden, will the subject of future work.

6 Discussion and Conclusions

The free surface multiple removal subseries predicts the correct time of all orders of multiple with just one term. It then takes a series to get the amplitudes of the second and higher order multiples correct. The internal multiple removal series takes one term to predict the right time, but a whole series to *approximate* the amplitudes of the multiples. Extending this analogue, we have now isolated an imaging subseries that requires an infinite number of terms to get the approximate depth. Clearly the subseries become more demanding the closer we get to reaching the ultimate objectives of direct inversion.

The derivation of the 1-D acoustic leading order imaging subseries algorithm presented in this paper constitutes a blueprint for deriving the algorithms in multi-D and extending them for more complicated Earth models. Significant progress has already been made in deriving the equations for variable velocity and density acoustic Earth models, and for a depth-varying reference medium (Zhang and Weglein, 2003; Liu and Weglein, 2003).

In conclusion, we have isolated a subseries of the inverse scattering series that images seismic data in depth in the absence of adequate velocity information. We have found analytically and numerically that this series' convergences properties are extremely favorable. The series images the reflectors directly at depths that are the leading order approximations to their precise locations. In 1-D, and for a constant density, varible velocity acoustic medium, there exists a closed form solution to this imaging subseries.

Acknowledgments

The first author would like to express his appreciation to Craig Cooper for his encouragement of this research. Kris Innanen and Tad Ulrych are thanked for valuable technical discussions. The support of the M-OSRP sponsors is gratefully acknowledged.

References

Berkhout, A. J. and D. W. V. Palthe (1981). Migration in terms of spatial deconvolution. *Geophysical Prospecting 27*, 261–291.

Carvalho, P. M. (1992). *Free-surface multiple reflection elimination method based on non-linear inversion of seismic data*. Ph. D. thesis, Universidade Federal da Bahia. in Portuguese.

Claerbout, J. F. (1971). Toward a unified theory of reflector mapping. *Geophysics 36*(3), 467–481.

Clayton, R. W. and R. H. Stolt (1981). A Born-WKBJ inversion method for acoustic reflection data. *Geophysics 46*(11), 1559–1567.

Gray, S. H., J. Etgen, J. Dellinger, and D. Whitmore (2001). Seismic migration problems and solutions. *Geophysics 66*(5), 1622–1640.

Liu, F. and A. B. Weglein (2003). Inverse series for a v(z) background. *Mission-Oriented Seismic Research Program 2*, 210–225.

Matson, K. H. (1997). *An inverse scattering series method for attenuating elastic multiples from multicomponent land and ocean bottom seismic data*. Ph. D. thesis, University of British Columbia.

Moses, H. (1956). Calculation of scattering potential from reflection coefficients. *Phys. Rev.* (102), 559–567.

Osen, A., B. G. Secrest, L. Amundsen, and A. Reitan (1998). Wavelet estimation from marine pressure measurements. *Geophysics 63*(6), 2108–2119.

Schneider, W. A. (1978). Integral formulation for migration in two-dimensions and three-dimensions. *Geophysics 43*(1), 49–76.

Stolt, R. H. (1978). Migration by Fourier transform. *Geophysics 43*(1), 23–48.

Stolt, R. H. and A. B. Weglein (1985). Migration and inversion of seismic data. *Geophysics 50*(12), 2458–2472.

Stork, C. and R. W. Clayton (1991). Linear aspects of tomographic velocity analysis. *Geophysics 56*(4), 483–495.

Tan, T. H. (1999). Wavelet spectrum estimation. *Geophysics 64*(6), 1836–1846.

Taner, M. T. and F. Koehler (1969). Velocity spectra - Digital computer derivation and applications of velocity functions. *Geophysics 34*(6), 859–881.

Tarantola, A. (1987). *Inverse problem theory*. Elsevier Science B.V.

Wapenaar, C. P. A., G. L. Peels, V. Budejicky, and A. J. Berkhout (1989). Inverse extrapolation of primary seismic waves. *Geophysics 54*(7), 853–863.

Weglein, A. B., W. E. Boyce, and J. E. Anderson (1981). Obtaining three-dimensional velocity information directly from reflection seismic data: An inverse scattering formalism. *Geophysics 46*(8), 1116–1120.

Weglein, A. B., F. A. Gasparotto, P. M. Carvalho, and R. H. Stolt (1997). An inverse-scattering series method for attenuating multiples in seismic reflection data. *Geophysics 62*(6), 1975–1989.

Weglein, A. B., K. H. Matson, D. J. Foster, P. M. Carvalho, D. Corrigan, and S. A. Shaw (2000). Imaging and inversion at depth without a velocity model: Theory, concepts and initial evaluation. In *70th Annual Internat. Mtg., Soc. Expl. Geophys., Expanded Abstracts*, pp. 1016–1019. Soc. Expl. Geophys.

Weglein, A. B., K. H. Matson, D. J. Foster, S. A. Shaw, P. M. Carvalho, and D. Corrigan (2002). Predicting the correct spatial location of reflectors without knowing or determining the precise medium and wave velocity: initial concept, algorithm and analytic and numerical example. *Journal of Seismic Exploration 10*, 367–382.

Weglein, A. B. and B. G. Secrest (1990). Wavelet estimation for a multidimensional acoustic or elastic earth. *Geophysics 55*(7), 902–913.

Zhang, H. and A. B. Weglein (2003). Target identification using the inverse scattering series; inversion of large-contrast, variable velocity and density acoustic media. *Mission-Oriented Seismic Research Program 2*, 196–209.

Ziolkowski, A. (1991). Why don't we measure seismic signatures? *Geophysics 56*(2), 190–201.

Appendix A: Solution for $\alpha_1(z)$

The first term in the inverse series for 1-D constant density acoustic media can be written

$$\psi(z_m;\omega) = \psi_0(z_m;\omega) + \int_{-\infty}^{\infty} G_0(z_m|z';\omega)k_0^2\alpha_1(z')\psi_0(z'|z_m;\omega)dz' \tag{A-1}$$

where

$$G_0(z_m|z';\omega) = \frac{e^{ik_0|z_m-z'|}}{2ik_0} \tag{A-2}$$

$$\psi_0(z'|z_m;\omega) = e^{ik_0(z'-z_m)} \tag{A-3}$$

$$\psi(z_m;\omega) - \psi_0(z_m;\omega) = \psi_s(z_m;\omega), \tag{A-4}$$

z_m is the measurement depth, and $k_0 = \omega/c_0$. The reference medium is chosen to be a homogeneous wholespace with velocity c_0 and the incident wavefield is written as a pseudo plane wave that passes depth z_m at time $t = 0$. Making use of the fact that all scattering points are below the measurement surface ($z' > z_m$)

$$\begin{aligned}\psi_s(z_m;\omega) &= k_0^2\int_{-\infty}^{\infty}\frac{e^{ik_0(z'-z_m)}}{2ik_0}\alpha_1(z')e^{ik_0(z'-z_m)}dz' \\ &= k_0^2\frac{e^{-2ik_0z_m}}{2ik_0}\int_{-\infty}^{\infty}\alpha_1(z')e^{2ik_0z'}dz'.\end{aligned} \tag{A-5}$$

So

$$\begin{aligned}\int_{-\infty}^{\infty}\alpha_1(z')e^{2ik_0z'}dz' &= \frac{-2\psi_s(z_m;\omega)}{ik_0}e^{2ik_0z_m} \\ &= -2c_0\frac{\psi_s(z_m;\omega)}{i\omega}e^{i\omega\tau} \text{ where } \tau = 2z_m/c_0\end{aligned} \tag{A-6}$$

Performing an inverse Fourier transform, we get

$$\begin{aligned}\alpha_1(z) &= \frac{-2}{c_0}\int_{-\infty}^{\infty}-2c_0\frac{\psi_s(z_m;\omega)}{i\omega}e^{i\omega(\tau-2z/c_0)}d\omega \\ &= 4\int_{-\infty}^{z}\psi_s(z_m;z')dz'\end{aligned} \tag{A-7}$$

where $z' = (c_0t/2 - z_m)$.

Appendix B: Separation of α_2 terms

The second term in the inverse series can be written

$$\int_{-\infty}^{\infty} G_0(z_g|z\,';k_0)k_0^2\alpha_2(z\,')\psi_0(z\,'|z_s;k_0)dz\,' =$$
$$-\int_{-\infty}^{\infty} G_0(z_g|z'';k_0)k_0^2\alpha_1(z'')\int_{-\infty}^{\infty} G_0(z''|z\,';k_0)k_0^2\alpha_1(z\,')\psi_0(z\,'|z_s;k_0)dz\,'dz'' \tag{B-1}$$

where

$$G_0(z_g|z\,';k_0) = \frac{e^{ik_0|z_g-z\,'|}}{2ik_0}$$
$$\psi_0(z\,'|z_s;k_0) = e^{ik_0(z\,'-z_s)}$$
$$k_0 = \omega/c_0$$

So

$$e^{-2ik_0z_m}\int_{-\infty}^{\infty}\frac{k_0^2}{2ik_0}\alpha_2(z\,')e^{2ik_0z\,'}dz\,' =$$
$$-\,e^{-2ik_0z_m}\int_{-\infty}^{\infty}\frac{k_0^4}{(2ik_0)^2}\alpha_1(z'')e^{ik_0z''}\int_{-\infty}^{\infty} e^{ik_0|z''-z\,'|}\alpha_1(z\,')e^{ik_0z\,'}dz\,'dz'' \tag{B-2}$$

As might be expected, the location of the measurment surface (z_m) cancels since this information is carried in α_1. Then cancelling some i's and k_0's yields

$$\frac{2}{ik_0}\int_{-\infty}^{\infty}\alpha_2(z\,')e^{2ik_0z\,'}dz\,' = \int_{-\infty}^{\infty}\alpha_1(z'')e^{ik_0z''}\int_{-\infty}^{\infty} e^{ik_0|z''-z\,'|}\alpha_1(z\,')e^{ik_0z\,'}dz\,'dz'' \tag{B-3}$$

and considering the absolute value in the exponential reveals a symmetry

$$\begin{aligned}\frac{2}{ik_0}\tilde{\alpha}_2(-2k_0) &= \int_{-\infty}^{\infty}\alpha_1(z'')e^{ik_0z''}\int_{-\infty}^{\infty} H(z''-z\,')e^{ik_0(z''-z\,')}\alpha_1(z\,')e^{ik_0z\,'}dz\,'dz''\\ &+\int_{-\infty}^{\infty}\alpha_1(z'')e^{ik_0z''}\int_{-\infty}^{\infty} H(z\,'-z'')e^{ik_0(z\,'-z'')}\alpha_1(z\,')e^{ik_0z\,'}dz\,'dz''\\ &= 2\int_{-\infty}^{\infty}\alpha_1(z'')e^{ik_0z''}\int_{-\infty}^{\infty} H(z\,'-z'')e^{ik_0(z\,'-z'')}\alpha_1(z\,')e^{ik_0z\,'}dz\,'dz''\end{aligned}$$

$$\tilde{\alpha}_2(-2k_0) = \int_{-\infty}^{\infty}\alpha_1(z'')\int_{-\infty}^{\infty} ik_0H(z\,'-z'')\alpha_1(z\,')e^{2ik_0z\,'}dz\,'dz'' \tag{B-4}$$

Integrating by parts

$$\begin{aligned}
u &= \int_{-\infty}^{\infty} \alpha_1(z'')H(z'-z'')\alpha_1(z')dz'' \\
dv &= ik_0 e^{2ik_0 z'}dz' \\
\frac{du}{dz'} &= \int_{-\infty}^{\infty} \alpha_1(z'')\left(\delta(z'-z'')\alpha_1(z') + H(z'-z'')\frac{d}{dz'}\alpha_1(z')\right)dz'' \\
&= \alpha_1^2(z') + \int_{-\infty}^{\infty}\left(\alpha_1(z'')H(z'-z'')\frac{d}{dz'}\alpha_1(z')\right)dz'' \\
v &= \frac{e^{2ik_0 z'}}{2}
\end{aligned}$$

Therefore,

$$\begin{aligned}
\tilde{\alpha}_2(-2k_0) = &\left[\int_{-\infty}^{\infty} \alpha_1(z'')H(z'-z'')\alpha_1(z')dz''\frac{e^{2ik_0 z'}}{2}\right]_{z'=-\infty}^{\infty} \\
&- \frac{1}{2}\left(\int_{-\infty}^{\infty} \alpha_1^2(z')e^{2ik_0 z'}dz'\right) \\
&- \frac{1}{2}\left(\int_{-\infty}^{\infty}\int_{-\infty}^{\infty} \alpha_1(z'')H(z'-z'')dz''\frac{d}{dz'}\left(\alpha_1(z')\right)e^{2ik_0 z'}dz'\right) \qquad \text{(B-5)}
\end{aligned}$$

The first term is taken to be zero under the assumption that the scattering potential is confined to some finite region $z_m < z' < \infty$. Then, performing an inverse Fourier transform on both sides yields

$$\boxed{\alpha_2(z) = -\frac{1}{2}\left(\alpha_1^2(z) + \left[\frac{d}{dz}\alpha_1(z)\right]\int_0^z \alpha_1(z')dz'\right)} \qquad \text{(B-6)}$$

Appendix C: Separation of α_3 terms

The third term in the inverse series can be written

$$\int_{-\infty}^{\infty} G_0(z_g, z'; k_0) k_0^2 \alpha_3(z') \psi_0(z'|z_s; k_0) dz' =$$
$$- \int_{-\infty}^{\infty} G_0(z_g, z''; k_0) k_0^2 \alpha_1(z'') \int_{-\infty}^{\infty} G_0(z'', z'; k_0) k_0^2 \alpha_2(z') \psi_0(z'|z_s; k_0) dz' dz''$$
$$- \int_{-\infty}^{\infty} G_0(z, z''; k_0) k_0^2 \alpha_2(z'') \int_{-\infty}^{\infty} G_0(z'', z'; k_0) k_0^2 \alpha_1(z') \psi_0(z'|z_s; k_0) dz' dz''$$
$$- \int_{-\infty}^{\infty} G_0(z, z'''; k_0) k_0^2 \alpha_1(z''') \int_{-\infty}^{\infty} G_0(z''', z''; k_0) k_0^2 \alpha_1(z'')$$
$$\times \int_{-\infty}^{\infty} G_0(z'', z'; k_0) k_0^2 \alpha_1(z') \psi_0(z'|z_s; k_0) dz' dz'' dz''' \tag{C-1}$$

which on substitution of G_0 and ψ_0 (Eqs. A-2 and A-3) reduces to

$$\tilde{\alpha}_3(-2k_0) = \tilde{I}_1 + \tilde{I}_2 + \tilde{I}_3 \tag{C-2}$$

where

$$\tilde{I}_1(-2k_0) = \frac{ik_0}{2} \int_{-\infty}^{\infty} \alpha_1(z'') e^{ik_0 z''} \int_{-\infty}^{\infty} e^{ik_0|z''-z'|} \alpha_2(z') e^{ik_0 z'} dz' dz''$$
$$\tilde{I}_2(-2k_0) = \frac{ik_0}{2} \int_{-\infty}^{\infty} \alpha_2(z'') e^{ik_0 z''} \int_{-\infty}^{\infty} e^{ik_0|z''-z'|} \alpha_1(z') e^{ik_0 z'} dz' dz''$$
$$\tilde{I}_3(-2k_0) = \frac{k_0^2}{4} \int_{-\infty}^{\infty} \alpha_1(z''') e^{ik_0 z'''} \int_{-\infty}^{\infty} e^{ik_0|z'''-z''|} \alpha_1(z'')$$
$$\times \int_{-\infty}^{\infty} e^{ik_0|z''-z'|} \alpha_1(z') e^{ik_0 z'} dz' dz'' dz'''$$

The first term can be expanded

$$\tilde{I}_1 = \tilde{I}_{11} + \tilde{I}_{12}$$

where

$$\tilde{I}_{11}(-2k_0) = \frac{ik_0}{2} \int_{-\infty}^{\infty} \alpha_1(z'') \int_{-\infty}^{\infty} H(z'' - z') \alpha_2(z') e^{2ik_0 z''} dz' dz''$$
$$\tilde{I}_{12}(-2k_0) = \frac{ik_0}{2} \int_{-\infty}^{\infty} \alpha_1(z'') \int_{-\infty}^{\infty} H(z' - z'') \alpha_2(z') e^{2ik_0 z'} dz' dz''$$

A symmetry exists between $\tilde{I}_1$ and $\tilde{I}_2$, since

$$\tilde{I}_2 = \tilde{I}_{21} + \tilde{I}_{22}$$

where

$$\tilde{I}_{21}(-2k_0) = \frac{ik_0}{2}\int_{-\infty}^{\infty} \alpha_2(z'')\int_{-\infty}^{\infty} H(z''-z')\alpha_1(z')e^{2ik_0z''}dz'dz''$$

$$\tilde{I}_{22}(-2k_0) = \frac{ik_0}{2}\int_{-\infty}^{\infty} \alpha_2(z'')\int_{-\infty}^{\infty} H(z'-z'')\alpha_1(z')e^{2ik_0z'}dz'dz''$$

we see that

$$\tilde{I}_{21} = \tilde{I}_{12}$$
$$\tilde{I}_{22} = \tilde{I}_{11}$$

so

$$\tilde{I}_2 = \tilde{I}_1. \qquad \text{(C-3)}$$

Integrating $\tilde{I}_{11}$ by parts provides

$$\begin{aligned}
u =& \alpha_1(z'')\int_{-\infty}^{\infty} H(z''-z')\alpha_2(z')dz' \\
dv =& \frac{ik_0 e^{2ik_0z''}}{2}dz'' \\
\frac{du}{dz''} =& \alpha_1(z'')\alpha_2(z'') + \int_{-\infty}^{z''}\alpha_2(z')dz'\left[\frac{d}{dz''}\left(\alpha_1(z'')\right)\right] \\
v =& \frac{e^{2ik_0z''}}{4} \\
\tilde{I}_{11}(-2k_0) =& \left[\frac{1}{4}\alpha_1(z'')\int_{-\infty}^{\infty} H(z''-z')\alpha_2(z')dz'e^{2ik_0z''}\right]_{z''=-\infty}^{\infty} \\
&- \frac{1}{4}\int_{-\infty}^{\infty}\alpha_1(z'')\alpha_2(z'')e^{2ik_0z''}dz'' \\
&- \frac{1}{4}\int_{-\infty}^{\infty}\int_{-\infty}^{z''}\alpha_2(z')dz'\left[\frac{d}{dz''}\left(\alpha_1(z'')\right)\right]e^{2ik_0z''}dz'' \qquad \text{(C-4)}
\end{aligned}$$

Similarly, integrating $\tilde{I}_{12}$ by parts yields

$$
\begin{aligned}
u =& \alpha_2(z') \int_{-\infty}^{\infty} H(z' - z'')\alpha_1(z'')dz'' \\
dv =& \frac{ik_0 e^{2ik_0 z'}}{2} dz' \\
\frac{du}{dz'} =& \alpha_2(z')\alpha_1(z') + \int_{-\infty}^{z'} \alpha_1(z'')dz'' \left[\frac{d}{dz'}\left(\alpha_2(z')\right)\right] \\
v =& \frac{e^{2ik_0 z'}}{4} \\
\tilde{I}_{12}(-2k_0) =& \left[\frac{1}{4}\alpha_2(z') \int_{-\infty}^{\infty} H(z' - z'')\alpha_1(z'')dz'' e^{2ik_0 z'}\right]_{z'=-\infty}^{\infty} \\
& - \frac{1}{4}\int_{-\infty}^{\infty} \alpha_2(z')\alpha_1(z') e^{2ik_0 z'} dz' \\
& - \frac{1}{4}\int_{-\infty}^{\infty}\int_{-\infty}^{z'} \alpha_1(z'')dz'' \left[\frac{d}{dz'}\left(\alpha_2(z')\right)\right] e^{2ik_0 z'} dz'
\end{aligned} \tag{C-5}
$$

Since the scattering potential is confined to a finite region, the boundary terms in Eqs. (C-4) and (C-5) are equal to zero. Then by Eq. (C-3),

$$
\begin{aligned}
\tilde{I}_1 + \tilde{I}_2 =& 2\tilde{I}_1 = 2\left(\tilde{I}_{11} + \tilde{I}_{12}\right) \\
=& -\frac{1}{2}\int_{-\infty}^{\infty} \alpha_1(z'')\alpha_2(z'') e^{2ik_0 z''} dz'' \\
& -\frac{1}{2}\int_{-\infty}^{\infty}\int_{-\infty}^{z''} \alpha_2(z')dz' \left[\frac{d}{dz''}\left(\alpha_1(z'')\right)\right] e^{2ik_0 z''} dz'' \\
& -\frac{1}{2}\int_{-\infty}^{\infty} \alpha_2(z')\alpha_1(z') e^{2ik_0 z'} dz' \\
& -\frac{1}{2}\int_{-\infty}^{\infty}\int_{-\infty}^{z'} \alpha_1(z'')dz'' \left[\frac{d}{dz'}\left(\alpha_2(z')\right)\right] e^{2ik_0 z'} dz'
\end{aligned}
$$

Performing an inverse Fourier transform $I_1(z') = \int_{-\infty}^{\infty} \tilde{I}_1(-2k_0) e^{2ik_0 z'} d(-2k_0)$ we have

$$
\begin{aligned}
I_1(z') + I_2(z') =& -\frac{1}{2}\alpha_1(z')\alpha_2(z') - \frac{1}{2}\int_{-\infty}^{z'} \alpha_2(z'')dz'' \left[\frac{d}{dz'}\left(\alpha_1(z')\right)\right] \\
& - \frac{1}{2}\alpha_2(z')\alpha_1(z') - \frac{1}{2}\int_{-\infty}^{z'} \alpha_1(z'')dz'' \left[\frac{d}{dz'}\left(\alpha_2(z')\right)\right] \\
=& -\alpha_1(z')\alpha_2(z') - \frac{1}{2}\int_{-\infty}^{z'} \alpha_2(z'')dz'' \left[\frac{d}{dz'}\left(\alpha_1(z')\right)\right] \\
& - \frac{1}{2}\int_{-\infty}^{z'} \alpha_1(z'')dz'' \left[\frac{d}{dz'}\left(\alpha_2(z')\right)\right]
\end{aligned} \tag{C-6}
$$

Recalling the expression for $\alpha_2(z')$

$$\alpha_2(z') = -\frac{1}{2}\alpha_1^2(z') - \frac{1}{2}\int_{-\infty}^{z'} \alpha_1(z'')dz'' \left[\frac{d}{dz'}\alpha_1(z')\right] \tag{C-7}$$

then to write Eq. C-6 in terms of only α_1 we need to integrate $\alpha_2(z')$:

$$\begin{aligned}\int_{-\infty}^{z''} \alpha_2(z')dz' = &-\frac{1}{2}\int_{-\infty}^{z''} \alpha_1^2(z')dz' \\ &-\frac{1}{2}\int_{-\infty}^{z''}\int_{-\infty}^{z'} \alpha_1(z''')dz''' \left[\frac{d}{dz'}\alpha_1(z')\right] dz'\end{aligned} \tag{C-8}$$

The second integral in Eq. (C-8) can be rewritten

$$-\frac{1}{2}\int_{-\infty}^{\infty} H(z''-z')\int_{-\infty}^{\infty} H(z'-z''')\alpha_1(z''')dz''' \left[\frac{d}{dz'}\alpha_1(z')\right] dz' \tag{C-9}$$

which can be integrated by parts

$$\begin{aligned}u =&H(z''-z')\int_{-\infty}^{\infty} H(z'-z''')\alpha_1(z''')dz''' \\ dv =&-\frac{1}{2}\frac{d}{dz'}\left(\alpha_1(z')\right)dz' \\ \frac{du}{dz'} =&H(z''-z')\int_{-\infty}^{\infty} \delta(z'-z''')\alpha_1(z''')dz''' \\ &-\delta(z''-z')\int_{-\infty}^{\infty} H(z'-z''')\alpha_1(z''')dz''' \\ =&H(z''-z')\alpha_1(z') - \delta(z''-z')\int_{-\infty}^{z'} \alpha_1(z''')dz''' \\ v =&-\frac{1}{2}\alpha_1(z')\end{aligned}$$

which leads to

$$\begin{aligned}\int_{-\infty}^{\infty} udv = &\left[-\frac{1}{2}\alpha_1(z')H(z''-z')\int_{-\infty}^{z'} \alpha_1(z''')dz'''\right]_{z'=-\infty}^{\infty} \\ &+\frac{1}{2}\int_{-\infty}^{\infty} \alpha_1(z')H(z''-z')\alpha_1(z')dz' \\ &-\frac{1}{2}\int_{-\infty}^{\infty} \delta(z''-z')\alpha_1(z')\int_{-\infty}^{z'} \alpha_1(z''')dz'''dz' \\ =&\frac{1}{2}\int_{-\infty}^{z''} \alpha_1^2(z')dz' - \frac{1}{2}\alpha_1(z'')\int_{-\infty}^{z''} \alpha_1(z''')dz'''.\end{aligned} \tag{C-10}$$

Therefore, the integral of $\alpha_2(z')$ (Eq.C-8) becomes

$$\int_{-\infty}^{z''} \alpha_2(z')dz' = -\frac{1}{2}\alpha_1(z'') \int_{-\infty}^{z''} \alpha_1(z''')dz'''. \tag{C-11}$$

It is interesting to see that the terms that are the integrals of α_1 squared cancel. To simplify Eq. (C-6), we also need to differentiate $\alpha_2(z')$:

$$\begin{aligned}
\left[\frac{d}{dz'}\alpha_2(z')\right] =& -\frac{1}{2}\left(2\alpha_1(z')\frac{d}{dz'}\alpha_1(z')\right) \\
& -\frac{1}{2}\left(\int_{-\infty}^{z'} \alpha_1(z'')dz'' \left[\frac{d^2}{dz'^2}\alpha_1(z')\right]\right) \\
& -\frac{1}{2}\frac{d}{dz'}\left(\int_{-\infty}^{\infty} H(z'-z'')\alpha_1(z'')dz''\right)\left[\frac{d}{dz'}\alpha_1(z')\right] \\
=& -\frac{3}{2}\alpha_1(z')\left[\frac{d}{dz'}\alpha_1(z')\right] \\
& -\frac{1}{2}\int_{-\infty}^{z'} \alpha_1(z'')dz'' \left[\frac{d^2}{dz'^2}\alpha_1(z')\right].
\end{aligned} \tag{C-12}$$

Therefore, substituting Eqs. (C-11) and (C-12) into Eq. (C-6), we have

$$\begin{aligned}
I_1(z') + I_2(z') =& \frac{1}{2}\alpha_1^3(z') + \frac{1}{2}\alpha_1(z')\int_{-\infty}^{z'} \alpha_1(z'')dz'' \left[\frac{d}{dz'}\alpha_1(z')\right] \\
& + \frac{1}{4}\alpha_1(z')\int_{-\infty}^{z'} \alpha_1(z'')dz'' \left[\frac{d}{dz'}\alpha_1(z')\right] \\
& + \frac{3}{4}\alpha_1(z')\int_{-\infty}^{z'} \alpha_1(z'')dz'' \left[\frac{d}{dz'}\alpha_1(z')\right] \\
& + \frac{1}{4}\left(\int_{-\infty}^{z'} \alpha_1(z'')dz''\right)^2 \left[\frac{d^2}{dz'^2}\alpha_1(z')\right]
\end{aligned}$$

$$\begin{aligned}
I_1(z) + I_2(z) =& \frac{1}{2}\alpha_1^3(z) + \frac{3}{2}\alpha_1(z)\int_{-\infty}^{z} \alpha_1(z')dz' \left[\frac{d}{dz}\alpha_1(z)\right] \\
& + \frac{1}{4}\left(\int_{-\infty}^{z} \alpha_1(z')dz'\right)^2 \left[\frac{d^2}{dz^2}\alpha_1(z)\right]
\end{aligned} \tag{C-13}$$

Now consider the third term in Eq. (C-2), namely

$$\tilde{I}_3 = \tilde{I}_{31} + \tilde{I}_{32} + \tilde{I}_{33} + \tilde{I}_{34}$$

where

$$\tilde{I}_{31}(-2k_0) = \frac{k_0^2}{4}\int_{-\infty}^{\infty}\alpha_1(z''')e^{2ik_0z'''}\int_{-\infty}^{\infty}H(z'''-z'')\alpha_1(z'') \times\int_{-\infty}^{\infty}H(z''-z')\alpha_1(z')dz'dz''dz''' \quad \text{(C-14)}$$

$$\tilde{I}_{32}(-2k_0) = \frac{k_0^2}{4}\int_{-\infty}^{\infty}\alpha_1(z''')\int_{-\infty}^{\infty}H(z''-z''')\alpha_1(z'')e^{2ik_0z''} \times\int_{-\infty}^{\infty}H(z''-z')\alpha_1(z')dz'dz''dz''' \quad \text{(C-15)}$$

$$\tilde{I}_{33}(-2k_0) = \frac{k_0^2}{4}\int_{-\infty}^{\infty}\alpha_1(z''')\int_{-\infty}^{\infty}H(z''-z''')\alpha_1(z'') \times\int_{-\infty}^{\infty}H(z'-z'')\alpha_1(z')e^{2ik_0z'}dz'dz''dz''' \quad \text{(C-16)}$$

$$\tilde{I}_{34}(-2k_0) = \frac{k_0^2}{4}\int_{-\infty}^{\infty}\alpha_1(z''')e^{2ik_0z'''}\int_{-\infty}^{\infty}H(z'''-z'')\alpha_1(z'')e^{-2ik_0z''} \times\int_{-\infty}^{\infty}H(z'-z'')\alpha_1(z')e^{2ik_0z'}dz'dz''dz''' \quad \text{(C-17)}$$

Equation (C-17) is equivalent to that for "W_{333}" (Eq. 5.8 in Matson (1997)), except for the substitution $V_1 = k_0^2\alpha_1$. The Heaviside functions in this equation ensure that $z''' > z''$ and $z' > z''$ so that the first and third scattering points are deeper than the second scattering point; hence the "W" diagram interpretation of the internal multiple attenuation algorithm. We will return to this equation a little later on.

Switching variables reveals that $\tilde{I}_{33} = \tilde{I}_{31}$. Notice that $k_0^2 = \frac{-(2ik_0)^2}{4}$ and performing an inverse Fourier transform over the conjugate variable $-2k_0$ yields

$$\begin{aligned}
I_3 =& 2I_{31} + I_{32} + I_{34} \\
=& -\frac{1}{8}\frac{d^2}{dz'''^2}\left(\alpha_1(z''')\int_{-\infty}^{\infty}\int_{-\infty}^{\infty}H(z'''-z'')\alpha_1(z'')H(z''-z')\alpha_1(z')dz'dz''\right) \\
& -\frac{1}{16}\frac{d^2}{dz'''^2}\left(\alpha_1(z''')\int_{-\infty}^{\infty}\int_{-\infty}^{\infty}H(z'''-z'')\alpha_1(z'')H(z'''-z')\alpha_1(z')dz'dz''\right) \\
& -\frac{1}{16}\frac{d^2}{dz'''^2}\left(\alpha_1(z''')\int_{-\infty}^{\infty}\int_{-\infty}^{\infty}H(z'''-z'')\alpha_1(z'')\right. \\
& \left.\times H(z'-z'')\alpha_1(z')e^{2ik_0z'}e^{-2ik_0z''}dz'dz''\right)
\end{aligned}$$

$$
\begin{aligned}
2I_{31}(z''') =& -\frac{1}{8}\frac{d}{dz'''}\left(\frac{d}{dz'''}\left(\alpha_1(z''')\right)\int_{-\infty}^{\infty}\right.\\
&\left.\times\int_{-\infty}^{\infty}H(z'''-z'')\alpha_1(z'')H(z''-z')\alpha_1(z')dz'dz''\right)\\
&-\frac{1}{8}\frac{d}{dz'''}\left(\alpha_1(z''')\int_{-\infty}^{\infty}\alpha_1(z''')H(z'''-z')\alpha_1(z')dz'\right)\\
=& -\frac{1}{8}\int_{-\infty}^{z'''}\alpha_1(z'')\int_{-\infty}^{z''}\alpha_1(z')dz'dz''\left[\frac{d^2}{dz'''^2}\alpha_1(z''')\right]\\
&-\frac{1}{8}\alpha_1(z''')\int_{-\infty}^{z'''}\alpha_1(z')dz'\left[\frac{d}{dz'''}\alpha_1(z''')\right]\\
&-\frac{1}{4}\alpha_1(z''')\int_{-\infty}^{z'''}\alpha_1(z')dz'\left[\frac{d}{dz'''}\alpha_1(z''')\right]-\frac{1}{8}\alpha_1^3(z''')\\
=& -\frac{1}{8}\int_{-\infty}^{z'''}\alpha_1(z'')\int_{-\infty}^{z''}\alpha_1(z')dz'dz''\left[\frac{d^2}{dz'''^2}\alpha_1(z''')\right]\\
&-\frac{3}{8}\alpha_1(z''')\int_{-\infty}^{z'''}\alpha_1(z')dz'\left[\frac{d}{dz'''}\alpha_1(z''')\right]-\frac{1}{8}\alpha_1^3(z''')
\end{aligned}
\tag{C-18}
$$

The nested integral in the first expression can be simplified as follows

$$
\begin{aligned}
u =& \int_{-\infty}^{z'}\alpha_1(z'')dz''\\
dv =& \alpha_1(z')\\
du =& \alpha_1(z')dz'\\
v =& \int_{-\infty}^{z'}\alpha_1(z'')dz''
\end{aligned}
$$

$$
\begin{aligned}
\int_{-\infty}^{z}\alpha_1(z')\int_{-\infty}^{z'}\alpha_1(z'')dz''dz' =& \left(\int_{-\infty}^{z'}\alpha_1(z'')dz''\right)^2\\
&-\int_{-\infty}^{z}\alpha_1(z')\int_{-\infty}^{z'}\alpha_1(z'')dz''dz'\\
=& \frac{1}{2}\left(\int_{-\infty}^{z'}\alpha_1(z'')dz''\right)^2
\end{aligned}
\tag{C-19}
$$

So equation (C-18) becomes

$$2I_{31}(z) = -\frac{1}{16}\left(\int_{-\infty}^{z}\alpha_1(z')dz'\right)^2\left[\frac{d^2}{dz^2}\alpha_1(z)\right] - \frac{3}{8}\alpha_1(z)\int_{-\infty}^{z}\alpha_1(z')dz'\left[\frac{d}{dz}\alpha_1(z)\right] - \frac{1}{8}\alpha_1^3(z) \tag{C-20}$$

and

$$\begin{aligned}
I_{32}(z''') =& -\frac{1}{16}\frac{d}{dz'''}\left(\frac{d}{dz'''}\left(\alpha_1(z''')\right)\left(\int_{-\infty}^{z'''}\alpha_1(z'')dz''\right)^2\right) \\
& -\frac{1}{8}\frac{d}{dz'''}\left(\alpha_1^2(z''')\int_{-\infty}^{z'''}\alpha_1(z'')dz''\right) \\
=& -\frac{1}{16}\left(\int_{-\infty}^{z'''}\alpha_1(z'')dz''\right)^2\left[\frac{d^2}{dz'''^2}\alpha_1(z''')\right] \\
& -\frac{2}{16}\alpha_1(z''')\int_{-\infty}^{z'''}\alpha_1(z'')dz''\left[\frac{d}{dz'''}\alpha_1(z''')\right] \\
& -\frac{1}{4}\alpha_1(z''')\int_{-\infty}^{z'''}\alpha_1(z')dz'\left[\frac{d}{dz'''}\alpha_1(z''')\right] \\
& -\frac{1}{8}\alpha_1^3(z''')
\end{aligned}$$

$$\begin{aligned}
I_{32}(z) =& -\frac{1}{16}\left(\int_{-\infty}^{z}\alpha_1(z')dz'\right)^2\left[\frac{d^2}{dz^2}\alpha_1(z)\right] \\
& -\frac{6}{16}\alpha_1(z)\int_{-\infty}^{z}\alpha_1(z')dz'\left[\frac{d}{dz}\alpha_1(z)\right] \\
& -\frac{1}{8}\alpha_1^3(z)
\end{aligned} \tag{C-21}$$

Finally, consider $\tilde{I}_{34}$ (Eq. C-17)

$$\begin{aligned}
\tilde{I}_{34}(-2k_0) =& -\frac{1}{16}\int_{-\infty}^{\infty}(2ik_0)^2\alpha_1(z''')\int_{-\infty}^{\infty}H(z'''-z'')\alpha_1(z'') \\
& \times\int_{-\infty}^{\infty}H(z'-z'')\alpha_1(z')e^{2ik_0(z'''-z''+z')}dz'dz''dz'''
\end{aligned}$$

and substitute $u = (z''' - z'' + z')$ to eliminate z''

$$\tilde{I}_{34}(-2k_0) = -\frac{1}{16}\int_{-\infty}^{\infty}(2ik_0)^2\alpha_1(z''')\int_{\infty}^{-\infty}H(u-z')\alpha_1(z'''+z'-u) \times \int_{-\infty}^{\infty}H(u-z''')\alpha_1(z')e^{2ik_0u}dz'(-du)dz'''$$

Notice that $dz'' = -du$ and the limits of integration of z'' and u are opposite. Switching the direction of the u integral introduces an overall minus sign. Performing an inverse Fourier transform yields

$$\begin{aligned}
I_{34}(u) = &-\frac{1}{16}\frac{\partial^2}{\partial u^2}\left(\int_{-\infty}^{\infty}\right. \\
&\times \left.\int_{-\infty}^{\infty}\alpha_1(z''')H(u-z')\alpha_1(z'''+z'-u)H(u-z''')\alpha_1(z')dz'dz'''\right) \\
= &-\frac{1}{16}\frac{\partial}{\partial u}\left(\int_{-\infty}^{\infty}\int_{-\infty}^{\infty}\alpha_1(z''')\right. \\
&\times \delta(u-z')\alpha_1(z'''+z'-u)H(u-z''')\alpha_1(z')dz'dz''') \\
&-\frac{1}{16}\frac{\partial}{\partial u}\left(\int_{-\infty}^{\infty}\int_{-\infty}^{\infty}\alpha_1(z''')\right. \\
&\times H(u-z')\alpha_1(z'''+z'-u)\delta(u-z''')\alpha_1(z')dz'dz''') \\
&-\frac{1}{16}\frac{\partial}{\partial u}\left(\int_{-\infty}^{\infty}\int_{-\infty}^{\infty}\alpha_1(z''')\right. \\
&\times \left. H(u-z')\frac{\partial}{\partial u}\left(\alpha_1(z'''+z'-u)\right)H(u-z''')\alpha_1(z')dz'dz'''\right) \\
= &-\frac{1}{16}\frac{\partial}{\partial u}\left(\int_{-\infty}^{\infty}\alpha_1^2(z''')H(u-z''')\alpha_1(u)dz'''\right) \\
&-\frac{1}{16}\frac{\partial}{\partial u}\left(\int_{-\infty}^{\infty}\alpha_1^2(z')H(u-z')\alpha_1(u)dz'\right) \\
&-\frac{1}{16}\frac{\partial}{\partial u}\left(\int_{-\infty}^{\infty}\int_{-\infty}^{\infty}\alpha_1(z''')\right. \\
&\times \left. H(u-z')\frac{\partial}{\partial u}\left(\alpha_1(z'''+z'-u)\right)H(u-z''')\alpha_1(z')dz'dz'''\right)
\end{aligned}$$

The first two expressions are equal and, when the differentiation is carried out, the last expression creates three integrals, two of which are also equal:

$$
\begin{aligned}
I_{34}(u) =& -\frac{1}{8}\alpha_1^3(u) - \frac{1}{8}\int_{-\infty}^{u} \alpha_1^2(z''')dz''' \left[\frac{\partial}{\partial u}\alpha_1(u)\right] \\
& - \frac{1}{16}\int_{-\infty}^{\infty}\int_{-\infty}^{\infty} H(u-z''')\alpha_1(z''')\delta(u-z\,')\alpha_1(z\,') \\
& \qquad \times \left[\frac{\partial}{\partial u}\alpha_1(z'''+z\,'-u)\right] dz\,'dz''' \\
& - \frac{1}{16}\int_{-\infty}^{\infty}\int_{-\infty}^{\infty} H(u-z\,')\alpha_1(z\,')\delta(u-z''')\alpha_1(z''') \\
& \qquad \times \left[\frac{\partial}{\partial u}\alpha_1(z'''+z\,'-u)\right] dz\,'dz''' \\
& - \frac{1}{16}\int_{-\infty}^{u}\int_{-\infty}^{u} \alpha_1(z''')\alpha_1(z\,') \left[\frac{\partial^2}{\partial u^2}\alpha_1(z'''+z\,'-u)\right] dz\,'dz'''
\end{aligned} \tag{C-22}
$$

Then summing the two integrals that are equal in Eq. (C-22) we get

$$
\begin{aligned}
2 \times & \left(-\frac{1}{16}\int_{-\infty}^{\infty}\int_{-\infty}^{\infty} H(u-z''')\alpha_1(z''')\delta(u-z\,')\alpha_1(z\,') \right. \\
& \qquad \left. \times \left[\frac{\partial}{\partial u}\alpha_1(z'''+z\,'-u)\right] dz\,'dz'''\right) \\
& = \frac{1}{8}\alpha_1(u)\int_{-\infty}^{\infty} H(u-z''')\alpha_1(z''')\left[\frac{d}{dz'''}\alpha_1(z''')\right] dz''' \\
& = \int_{-\infty}^{\infty} pdq
\end{aligned} \tag{C-23}
$$

where

$$
\begin{aligned}
p =& \alpha_1(z''')H(u-z''') \\
dq =& \frac{1}{8}\alpha_1(u)\left[\frac{d}{dz'''}\alpha_1(z''')\right] \\
\frac{dp}{dz'''} =& \left[\frac{d}{dz'''}\alpha_1(z''')\right] H(u-z''') - \alpha_1(z''')\delta(u-z''') \\
q =& \frac{1}{8}\alpha_1(u)\alpha_1(z''')
\end{aligned}
$$

Notice that the change in sign in Eq. (C-23) reflects the fact that the derivative with respect to u was carried out before the delta function acted on it. Since α_1 was a function of $-u$, then a minus sign was introduced. Then

$$\begin{aligned}\int_{-\infty}^{\infty} pdq =&0-\frac{1}{8}\alpha_1(u)\int_{-\infty}^{\infty} H(u-z''')\alpha_1(z''')\left[\frac{d}{dz'''}\alpha_1(z''')\right]dz''' \\ &+\frac{1}{8}\alpha_1(u)\int_{-\infty}^{\infty}\alpha_1^2(z''')\delta(u-z''')dz''' \\ =&-\int_{-\infty}^{\infty} p\ dq+\frac{1}{8}\alpha_1^3(u) \\ =&\frac{1}{16}\alpha_1^3(u)\end{aligned} \tag{C-24}$$

Substituting Eq. (C-24) into Eq. (C-22) yields

$$\begin{aligned}I_{34}(u)=&-\frac{1}{16}\alpha_1^3(u)-\frac{1}{8}\int_{-\infty}^{u}\alpha_1^2(z''')dz'''\left[\frac{\partial}{\partial u}\alpha_1(u)\right] \\ &-\frac{1}{16}\int_{-\infty}^{u}\int_{-\infty}^{u}\alpha_1(z''')\alpha_1(z')\left[\frac{\partial^2}{\partial u^2}\alpha_1(z'''+z'-u)\right]dz'dz'''\end{aligned} \tag{C-25}$$

The last term in this equation can be integrated by parts:

$$I_{343}(u)=-\frac{1}{16}\int_{-\infty}^{\infty} H(u-z''')\alpha_1(z''')\int_{-\infty}^{\infty} p\ dq\ dz''' \tag{C-26}$$

where

$$\begin{aligned}p&=H(u-z')\alpha_1(z') \\ dq&=\left[\frac{\partial^2}{\partial u^2}\alpha_1(z'''+z'-u)\right]dz' \\ \frac{dp}{dz'}&=H(u-z')\frac{d}{dz'}\alpha_1(z')-\delta(u-z')\alpha_1(z') \\ q&=-\left[\frac{\partial}{\partial u}\alpha_1(z'''+z'-u)\right]\end{aligned}$$

The boundary values are zero:

$$[p\ q]_{z'=-\infty}^{\infty}=\left[-H(u-z')\alpha_1(z')\frac{\partial}{\partial u}\alpha_1(z'''+z'-u)\right]_{z'=-\infty}^{\infty}=0 \tag{C-27}$$

so Eq. (C-26) becomes

$$
\begin{aligned}
&I_{343}(u) = 0 \\
&-\frac{1}{16}\int_{-\infty}^{\infty} H(u-z''')\alpha_1(z''')\left[\int_{-\infty}^{u} \frac{d}{dz'}\left(\alpha_1(z')\right)\frac{\partial}{\partial u}\alpha_1(z'''+z'-u)dz'\right]dz''' \\
&+\frac{1}{16}\int_{-\infty}^{\infty} H(u-z''')\alpha_1(z''')\left[\int_{-\infty}^{\infty} \delta(u-z')\alpha_1(z')\frac{\partial}{\partial u}\alpha_1(z'''+z'-u)dz'\right]dz''' \\
&=-\frac{1}{16}\int_{-\infty}^{u} \frac{d}{dz'}\left(\alpha_1(z')\right)\int_{-\infty}^{\infty} H(u-z''')\alpha_1(z''')\frac{\partial}{\partial u}\alpha_1(z'''+z'-u)dz'''dz' \\
&\quad-\frac{1}{16}\alpha_1(u)\int_{-\infty}^{u} \alpha_1(z''')\frac{d}{dz'''}\alpha_1(z''')dz''' \\
&=-\frac{1}{16}\int_{-\infty}^{u} \frac{d}{dz'}\left(\alpha_1(z')\right)\int_{-\infty}^{\infty} H(u-z''')\alpha_1(z''')\frac{\partial}{\partial u}\alpha_1(z'''+z'-u)dz'''dz' \\
&\quad-\frac{1}{32}\alpha_1^3(u)
\end{aligned}
\qquad \text{(C-28)}
$$

As before, the derivative with respect to u was carried out before the integration with the delta function, which introduced the change in sign. Now performing the z''' integration (Eq. C-28) by parts in the same fashion gives

$$
\int_{-\infty}^{\infty} H(u-z''')\alpha_1(z''')\frac{\partial}{\partial u}\alpha_1(z'''+z'-u)dz''' = \int_{-\infty}^{\infty} p\ dq
$$

where

$$
\begin{aligned}
p &= H(u-z''')\alpha_1(z''') \\
dq &= \frac{\partial}{\partial u}\alpha_1(z'''+z'-u)dz''' \\
\frac{dp}{dz'''} &= H(u-z''')\frac{d}{dz'''}\alpha_1(z''') - \delta(u-z''')\alpha_1(z''') \\
q &= -\alpha_1(z'''+z'-u)
\end{aligned}
\qquad \text{(C-29)}
$$

So

$$
\begin{aligned}
\int_{-\infty}^{\infty} p\ dq =& 0 + \left[\int_{-\infty}^{u} \frac{d}{dz'''}\left(\alpha_1(z''')\right)\alpha_1(z'''+z'-u)dz'''\right] \\
&-\left[\int_{-\infty}^{\infty} \delta(u-z''')\alpha_1(z''')\alpha_1(z'''+z'-u)dz'''\right] \\
=& \left[\int_{-\infty}^{u} \frac{d}{dz'''})\alpha_1(z''')\right)\alpha_1(z'''+z'-u)dz'''\right] - \alpha_1(u)\alpha_1(z')
\end{aligned}
$$

and inserting this expression into Eq. (C-28) gives

$$
\begin{aligned}
I_{343} = &-\frac{1}{16}\int_{-\infty}^{u}\frac{d}{dz'}\left(\alpha_1(z')\right)\left[\int_{-\infty}^{u}\frac{d}{dz'''}\alpha_1(z''')\alpha_1(z'''+z'-u)dz'''\right]dz' \\
&+\frac{1}{16}\alpha_1(u)\int_{-\infty}^{u}\alpha_1(z')\frac{d}{dz'}\alpha_1(z')dz'+\frac{1}{32}\alpha_1^3(u) \\
=&-\frac{1}{16}\int_{-\infty}^{u}\int_{-\infty}^{u}\frac{d}{dz'}\left(\alpha_1(z')\right)\frac{d}{dz'''}\left(\alpha_1(z''')\right)\alpha_1(z'''+z'-u)dz'''dz' \\
&-\frac{1}{32}\alpha_1^3(u)+\frac{1}{32}\alpha_1^3(u)
\end{aligned}
\qquad \text{(C-30)}
$$

which, when substituted into Eq. (C-25), gives the last piece of the $G_0V_1G_0V_1G_0V_1\psi_0$ term

$$
\begin{aligned}
I_{34}(z) = &-\frac{1}{16}\alpha_1^3(z)-\frac{1}{8}\int_{-\infty}^{z}\alpha_1^2(z')dz'\left[\frac{\partial}{\partial z}\alpha_1(z)\right] \\
&-\frac{1}{16}\int_{-\infty}^{z}\int_{-\infty}^{z}\frac{d}{dz'}\left(\alpha_1(z')\right)\frac{d}{dz''}\left(\alpha_1(z'')\right)\alpha_1(z''+z'-z)dz''dz'
\end{aligned}
\qquad \text{(C-31)}
$$

Finally, summing Eqs. (C-13), (C-20), (C-21) and (C-31), yields

$$
\begin{aligned}
\alpha_3(z) =&I_1(z)+I_2(z)+I_3(z)=2I_1+I_{31}+I_{32}+I_{33}+I_{34} \\
=&2I_1+2I_{31}+I_{32}+I_{34} \\
=&(\text{Eq. C-13})+(\text{Eq. C-20})+(\text{Eq. C-21})+(\text{Eq. C-31}) \\
=&\frac{1}{2}\alpha_1^3(z)+\frac{3}{2}\alpha_1(z)\int_{-\infty}^{z}\alpha_1(z')dz'\left[\frac{d}{dz}\alpha_1(z)\right] \\
&+\frac{1}{4}\left(\int_{-\infty}^{z}\alpha_1(z')dz'\right)^2\left[\frac{d^2}{dz^2}\alpha_1(z)\right] \\
&-\frac{1}{16}\left(\int_{-\infty}^{z}\alpha_1(z')dz'\right)^2\left[\frac{d^2}{dz^2}\alpha_1(z)\right] \\
&-\frac{3}{8}\alpha_1(z)\int_{-\infty}^{z}\alpha_1(z')dz'\left[\frac{d}{dz}\alpha_1(z)\right]-\frac{1}{8}\alpha_1^3(z) \\
&-\frac{1}{16}\left(\int_{-\infty}^{z}\alpha_1(z')dz'\right)^2\left[\frac{d^2}{dz^2}\alpha_1(z)\right] \\
&-\frac{6}{16}\alpha_1(z)\int_{-\infty}^{z}\alpha_1(z')dz'\left[\frac{d}{dz}\alpha_1(z)\right]-\frac{1}{8}\alpha_1^3(z) \\
&-\frac{1}{16}\alpha_1^3(z)-\frac{1}{8}\int_{-\infty}^{z}\alpha_1^2(z')dz'\left[\frac{d}{dz}\alpha_1(z)\right] \\
&-\frac{1}{16}\int_{-\infty}^{z}\int_{-\infty}^{z}\frac{d}{dz'}\left(\alpha_1(z')\right)\frac{d}{dz''}\left(\alpha_1(z'')\right)\alpha_1(z''+z'-z)dz''dz'
\end{aligned}
\qquad \text{(C-32)}
$$

There are four $\alpha_1^3(z')$ terms, three terms that are $\alpha_1 \int \alpha_1 [\alpha_1']$ and three terms that are $(\int \alpha_1)^2 [\alpha_1'']$. Summing up, Eq. (C-32) reduces to

$$\begin{aligned}\alpha_3(z) =& \frac{3}{16}\alpha_1^3(z) + \frac{3}{4}\alpha_1(z)\int_{-\infty}^{z} \alpha_1(z')dz' \left[\frac{d}{dz}\alpha_1(z)\right] \\ &+ \frac{1}{8}\left(\int_{-\infty}^{z} \alpha_1(z')dz'\right)^2 \left[\frac{d^2}{dz^2}\alpha_1(z)\right] \\ &- \frac{1}{8}\int_{-\infty}^{z} \alpha_1^2(z')dz' \left[\frac{d}{dz}\alpha_1(z)\right] \\ &- \frac{1}{16}\int_{-\infty}^{z}\int_{-\infty}^{z} \left[\frac{d}{dz'}\alpha_1(z')\right]\left[\frac{d}{dz''}\alpha_1(z'')\right]\alpha_1(z''+z'-z)dz''dz' \end{aligned} \qquad \text{(C-33)}$$

The *leading* order (LO) inverse series imaging term in α_3 is

$$\alpha_3^{IS_{LO}}(z) = \frac{1}{8}\left(\int_{-\infty}^{z} \alpha_1(z')dz'\right)^2 \left[\frac{d^2}{dz^2}\alpha_1(z)\right]$$

which produce the expected coefficients for a known analytic data example. $\alpha_3^{IS_{LO}}$ is contributed to by all three componenents of the third term of the inverse series, i.e., $G_0V_2G_0V_1\psi_0$, $G_0V_1G_0V_2\psi_0$ and $G_0V_1G_0V_1G_0V_1\psi_0$.